Sphoorti Srivastava [1]
Neeraj Mehta [2]
Deepak Kumar [3]
Ashok Kumar [1]

[1] *Department of Physics, Harcourt Butler Technological Institute, Kanpur – 02, INDIA*
[2] *Department of Physics, Banaras Hindu University, Varanasi, India*
[3] *Department of Physics, J. S. S. Academy of Technical Education, Noida, INDIA*

Crystallization and Glass Transition Kinetics in $Se_{90}Sb_{10-x}Ag_x$ Glassy Alloys

Alloys of $Se_{100-x}Sb_{10-x}Ag_x$ (x=2, 4, 8) glassy system are obtained with rapid quenching. Calorimetric studies have been performed at different heating rates under non-isothermal conditions. Well defined endothermic and exothermic peaks are obtained at glass transition (T_g) and crystallization temperatures (T_c). In the present study, the glassy alloys are found to have double glass transition and crystallization temperatures. From the dependence of the glass transition temperature on the heating rate β, the activation energy of glass transition has been calculated on the basis of Moynihan and Kissinger models. The value of (T_c–T_g) and stability parameters have also been calculated for each composition for both the phases. Value of E_g is found to be decreased with increase in concentration of Ag. The values of (T_c-T_g) is highest for the sample with 8 at % of Ag. Activation energy of crystallization (E_c) has also been calculated using the well-known Kissinger's relation, Matusita–Sakka theory and the method of Augis and Bennett. A good agreement has been found in all the three methods. The activation energy of crystallization is found to decrease with increasing concentration of Ag.

Keywords: Chalcogenide Glasses, Differential scanning, Calorimetry, Transition kinetics
Received: 14 January 2013, Accepted: 2 February 2013

1. Introduction

Differential Scanning Calorimetery (DSC) is more sensitive than other thermoanalytical technique, Differential Thermal Analysis (DTA), and measures the volume fraction transferred as a function of time and temperature by measuring the heat liberated or absorbed during the phase change. The study of crystallization kinetics using DSC has been widely discussed in the literature [1 - 5]. DSC is widely used to study the dependence of glass transition temperature (T_g) and crystallization temperature (T_c) on the particle size, composition and heating rate. From the heating rate dependence of glass transition and crystallization temperatures the activation energies of glass transition and crystallization are calculated. Thermally activated transformations in the solid state can be investigated by isothermal or non-isothermal experiments [6 - 8]. In the isothermal method, the sample is brought quickly to a temperature above T_g and the heat evolved during the crystallization process is recorded as a function of time. Compared with isothermal techniques, non-isothermal experiments can be performed over a shorter time period and over a wider temperature range. In addition many phase transformations occur too rapidly to be measured under isothermal conditions because of the inherent transients associated with the experimental apparatus [6]. In the non-isothermal method, the sample is heated at a fixed rate and the heat evolved is again recorded as a function of temperature or time. A constant heating rate method (non-isothermal method) does not have the drawback of isothermal method [9], i.e., the impossibility of reaching a test temperature instantaneously and during the time in which the system needs to stabilize no measurements are possible. In general, therefore, crystallization studies have been made under non-isothermal conditions with the sample heated at several uniform heating rates. So, in the present study also, an effort has been made to determine the activation energies of glass transition and crystallization by using heating rate dependence of the T_g and T_c.

Thin films of chalcogenide glasses containing Ag have found application in erasable PC optical recording [10-15]. Different Ag doped chalcogenide alloys have been developed as recording layer and their good practical performance have been reported [10-15]. The electrical, optical and structural properties of Ag doped chalcogenide glasses have been studied by various workers [16-25] but there are only a few studies reported on crystallization kinetics in these materials [26-28].

Generally, silver containing chalcogenide glasses, exhibit single glass transition and single crystallization temperature, but in the present study the glassy alloys of $Se_{90}Sb_{10-x}Ag_x$ (x=2, 4, 8) are found to have double glass transition and crystallization temperatures. Therefore, crystallization kinetics of these glassy alloys has been studied in detail for both the phases present in these alloys.

2. Experimental Procedure

Glassy alloys of $Se_{90}Sb_{10-x}Ag_x$ (x=2, 4, 8) were prepared by quenching technique. The exact proportions of high purity (99.999%) elements, in

accordance with their atomic percentages, were weighed using an electronic balance (LIBROR. AEG -120), with the least count 10^{-4} mg. The materials were then sealed in evacuated (~10^{-5} torr) quartz ampoules (length ~5cm and internal diameter ~8mm). Each ampoule was kept inside the furnace at 1000°C temperature (where the temperature was raised at a rate of 3-4°C⁄min.). During heating, all the ampoules were constantly rocked by rotating a ceramic rod to which the ampoules were tucked away in the furnace. This was done to obtain homogeneous glassy alloys.

After rocking for about 10 hours, the obtained melts were cooled rapidly by removing them from the furnace and dropping them to ice-cooled water rapidly. The ingots of the samples were then taken out by breaking the quartz ampoules.

The glasses thus prepared, were ground to make fine powder for DSC studies. Here, 10 to 20 mg of the powder was heated at constant heating rate and the changes in heat flow with respect to an empty reference pan were measured. DSC plus instrument (Rheometric Scientific Company, U.K.) was used at four different heating rates of 5, 10, 15 and 20°C/min.

3. Results and Discussion

Figures (1) and (2) show typical DSC thermograms for glassy $Se_{90}Sb_{10-x}Ag_x$ (x=2, 4 and 8) at heating rate 15 K/min. Similar thermograms were obtained for other heating rates also (not shown here). These figures indicate that two phases occur simultaneously during glass transition region and crystalline transition region.

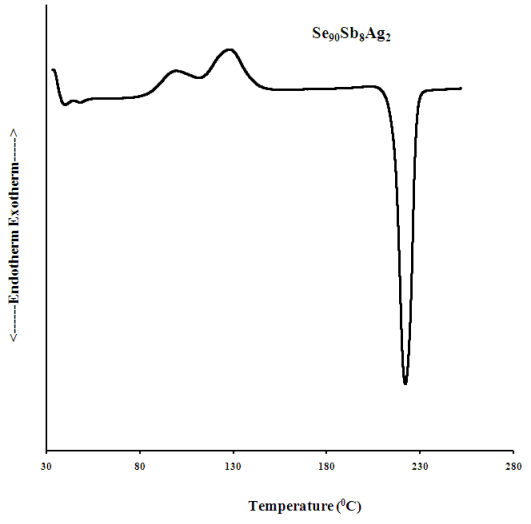

Fig. (1) DSC thermogram for glassy $Se_{90}Sb_8Ag_2$ alloy for heating rate 15°C/min

3.1 Composition Dependence of Glass Transition and Crystallization Temperature

Tables (1) and (2) give the values of glass transition temperature for different compositions at various heating rates. From the given data it is clear that glass transition temperature increases with Ag concentration for phase two. However, for phase one there is no drastic change in T_g with composition.

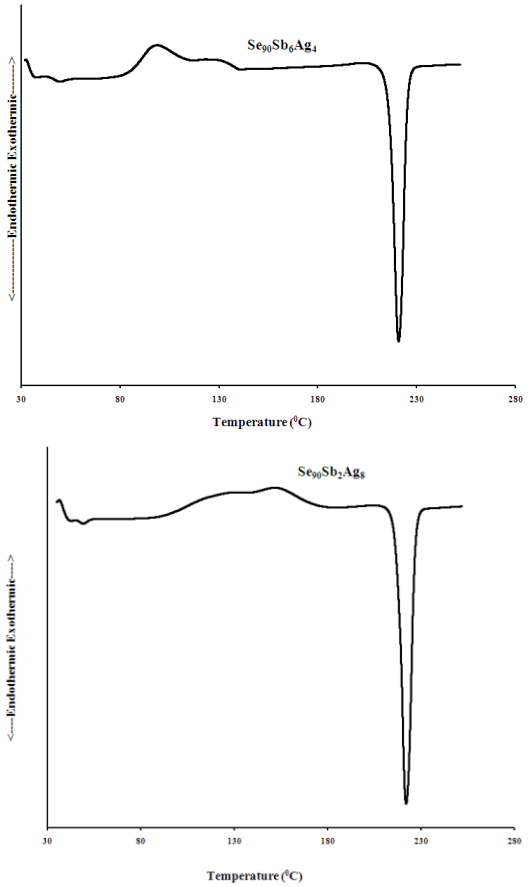

Fig. (2) DSC thermogram for glassy $Se_{90}Sb_6Ag_4$ and $Se_{90}Sb_2Ag_8$ alloy for heating rate 15°C/min

Table (1) Glass transition temperature T_{g1} at different heating rates for phase 1

Heating rate	$Se_{90}Sb_8Ag_2$	$Se_{90}Sb_6Ag_4$	$Se_{90}Sb_2Ag_8$
5 K/min	309.69	309.53	307.01
10 K/min	312.01	312.15	311.53
15 K/min	313.06	310.8	315.64
20 K/min	313.30	314.7	313.11

Table (2) Glass transition temperature T_{g2} at different heating rates for phase 2

Heating rate	$Se_{90}Sb_8Ag_2$	$Se_{90}Sb_6Ag_4$	$Se_{90}Sb_2Ag_8$
5 K/min	317.69	318.35	318.61
10 K/min	318.99	320.12	320.95
15 K/min	321.06	322.58	322.19
20 K/min	323.19	323.43	324.17

Tables (3) and (4) give the variation of crystallization temperature for different

compositions at various heating rates. It is clear from these tables that crystallization temperature increases with the increase in heating rate. These values are also composition dependent.

Table (3) Crystallization temperature T_{c1} at different heating rates for phase 1

Heating Rate	$Se_{90}Sb_8Ag_2$	$Se_{90}Sb_6Ag_4$	$Se_{90}Sb_2Ag_8$
5^0C/min	363.04	360.75	401.23
10^0C/min	366.98	367.33	414.41
15^0C/min	372.46	371.66	402.73
20^0C/min	373.92	374.13	404.70

Table (4) Crystallization temperature T_{c2} at different heating rates for phase 2

Heating Rate	$Se_{90}Sb_8Ag_2$	$Se_{90}Sb_6Ag_4$	$Se_{90}Sb_2Ag_8$
5^0C/min	388.51	391.28	---
10^0C/min	393.52	396.45	---
15^0C/min	401.09	397	424.62
20^0C/min	397.75	397.93	431.37

3.2 Activation Energy of Glass Transition

The evaluation of activation energy of glass transition (E_g) from the heating rate dependence of glass transition temperature is widely used in the literature. The theory of glass transition kinetics and structural relaxation as developed by Moynihan and other workers [29-31] has been used for this purpose. According to this theory, T_g and heating rate β are related as per the following equation:

$$\frac{d\,Ln\beta}{d\left(\frac{1}{T_g}\right)} = -\frac{E_g}{R} \qquad (1)$$

According to Eq. (1), the ln β versus $1/T_g$ plot should be a straight line and the activation energy involved in the molecular motions and rearrangements around T_g can be calculated from the slope of the plot of ln β vs. $10^3 / T_g$.

Kissinger's method is most commonly used in analyzing crystallization data of DSC experiment. Kissinger showed that:

$$Ln\left(\frac{\beta}{T_c^2}\right) = Constant - \frac{E_c}{RT_c} \qquad (2)$$

where T_c is peak crystallization temperature

Although originally derived for the crystallization process, it is suggested that this relation is valid for glass transition process [32 - 33] also and hence the above equation takes the following form for its use in glass transition kinetics:

$$Ln\left(\frac{\beta}{T_g^2}\right) = -\frac{E_g}{RT_g} + Constant \qquad (3)$$

Using Moynihan's relation, equation (1), the plots of ln β against $10^3/T_g$ are plotted for various glassy alloys. These plots are shown in Figs. (3-8) for various glassy alloys of $Se_{90}Sb_{10-x}Ag_x$ (x=2, 4, 8). The slopes of these plots are used to calculate the activation energy of glass transition process. Tables (5) and (6) show the E_g values obtained from Eq. (1). The values of E_g are also evaluated from the slopes of plots of ln (β/T_g^2) against $10^3/T_g$ for various glassy systems using Kissinger's relation, i.e., Eq. (3). The plots of ln (β/T_g^2) vs. $1000 / T_g$ are also shown in Figs. (3-8) for glassy alloys of $Se_{90}Sb_{10-x}Ag_x$ (x=2, 4, 8). These values of E_g are given in Tables (5) and (6) for both phases.

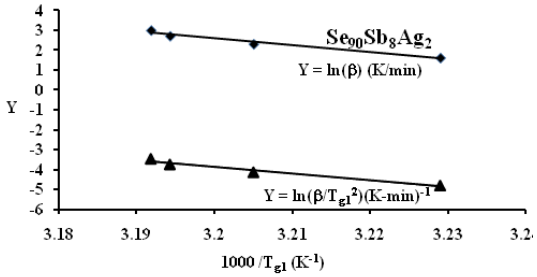

Fig. (3) Plots of $\ln(\beta/T_{g1}^2)$, $\ln(\beta)$ against $10^3/T_{g1}$ for $Se_{90}Sb_8Ag_2$

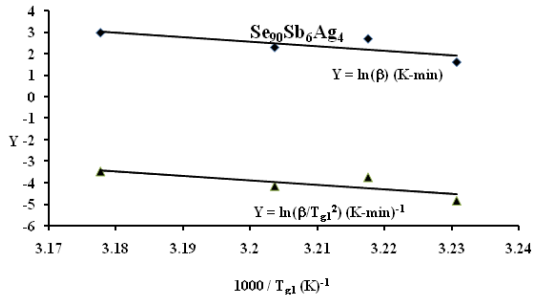

Fig. (4) Plots of $\ln(\beta/T_{g1}^2)$, $\ln(\beta)$ against $10^3/T_{g1}$ for $Se_{90}Sb_6Ag_4$

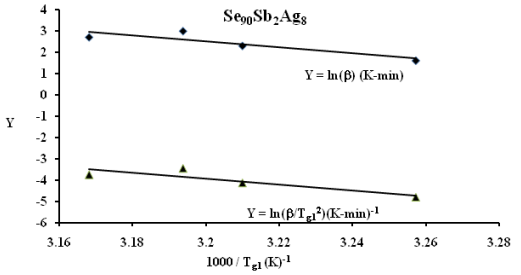

Fig. (5) Plots of $\ln(\beta/T_{g1}^2)$, $\ln(\beta)$ against $10^3/T_{g1}$ for $Se_{90}Sb_2Ag_8$

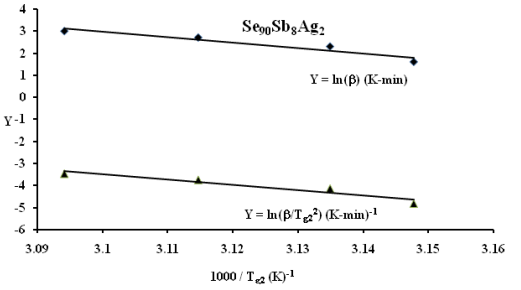

Fig. (6) Plots of $\ln(\beta/T_{g2}^2)$, $\ln(\beta)$ against $10^3/T_{g2}$ for $Se_{90}Sb_8Ag_2$

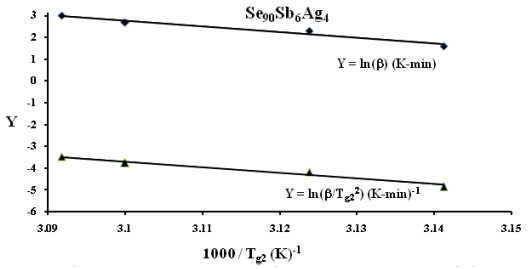

Fig. (7) Plots of $\ln(\beta/T_{g2}^2)$, $\ln(\beta)$ against $10^3/T_{g2}$ for $Se_{90}Sb_6Ag_4$

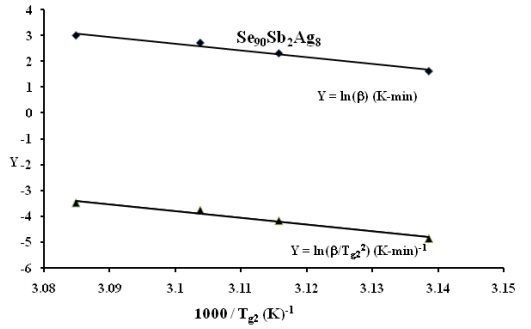

Fig. (8) Plots of $\ln(\beta/T_{g2}^2)$, $\ln(\beta)$ against $10^3/T_{g2}$ for $Se_{90}Sb_2Ag_8$

It is evident from the Tables (5) and (6) and Figs. (9) and (10) that E_g varies with Ag concentration and decreases as Ag concentration increases. It can be explained in terms of atomic weights of Sb and Ag. The atomic weight of Ag (107.87 gm/mol) is much less than that of Sb (121.75 gm/mol). In the present case, Ag is added in binary $Se_{90}Sb_{10}$ at the cost of Sb. Thus, the mean atomic weight of ternary alloys is decreased. This may probably be the reason why activation energy of glass transition is lower as Ag concentration increases.

Table (5) Activation Energy of glass transition E_{g1} (eV) for various glassy alloys of $Se_{90}Sb_{10-x}Ag_x$ for phase 1

Sample	Moynihan's relation	Kissinger's relation
$Se_{90}Sb_8Ag_2$	1.96	1.93
$Se_{90}Sb_6Ag_4$	1.82	1.79
$Se_{90}Sb_2Ag_8$	1.22	1.19

Table (6) Activation Energy of glass transition E_{g2} (eV) for various glassy alloys of $Se_{90}Sb_{10-x}Ag_x$ for phase 2

Sample	Moynihan's relation	Kissinger's relation
$Se_{90}Sb_8Ag_2$	1.99	1.96
$Se_{90}Sb_6Ag_4$	1.89	1.86
$Se_{90}Sb_2Ag_8$	1.79	1.77

Table (7) Values of T_{c1}–T_{g1} for various glassy alloys of $Se_{90}Sb_{10-x}Ag_x$

Heating Rate	$Se_{90}Sb_8Ag_2$	$Se_{90}Sb_6Ag_4$	$Se_{90}Sb_2Ag_8$
5^0C/min	53.35	51.22	94.22
10^0C/min	56.89	55.18	99.58
15^0C/min	58.4	60.86	88.09
20^0C/min	60.84	59.43	92.88

Table (8) Values of T_{c2}–T_{g2} for various glassy alloys of $Se_{90}Sb_{10-x}Ag_x$

Heating Rate	$Se_{90}Sb_8Ag_2$	$Se_{90}Sb_6Ag_4$	$Se_{90}Sb_2Ag_8$
5^0C/min	72.02	71.93	-
10^0C/min	75.53	77.65	-
15^0C/min	77.95	72.42	101.20
20^0C/min	73.56	75.50	106.97

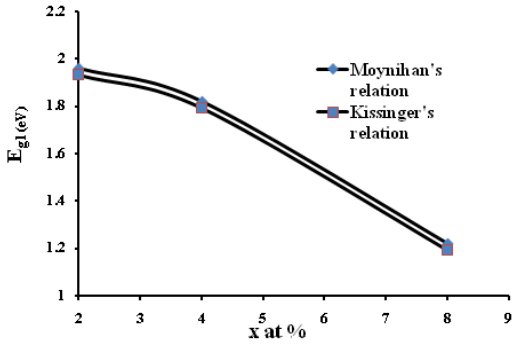

Fig. (9) E_{g1} vs. atomic percentage of Ag in glassy $Se_{90}Sb_{10-x}Ag_x$

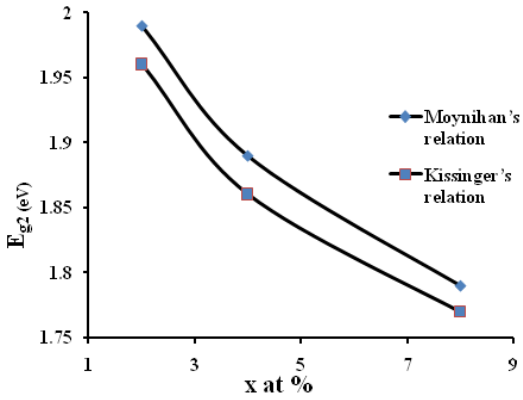

Fig. (10) E_{g2} vs. atomic percentage of Ag in glassy $Se_{90}Sb_{10-x}Ag_x$

3.3 Thermal Stability of Glassy $Se_{90}Sb_{10-x}Ag_x$ (x=2, 4, 8)

It has been found that the difference of T_c and T_g is a strong indicator of both the thermal stability and GFT. The higher the values of (T_c-T_g), the greater is the GFT, because the higher the value of this difference, the more the delay in the nucleation process [34]. Tables (1-4) show the glass transition and crystallization temperature T_c at various heating rates for phase one and two in all the glasses studied. Values of difference of glass transition temperature (T_g) and crystallization temperature (T_c) are given in Tables (9) and (10) for both the phases. Figures (11) and (12) show the variation of (T_c-T_g) with concentration of Ag for both phases. It is clear that (T_c-T_g) increases with Ag concentration. This indicates that thermal stability is higher at higher concentration of Ag.

Table (9) Activation energy of crystallization E_{c1}(eV) in various glassy alloys of $Se_{90}Sb_{10-x}Ag_x$

Non-isothermal Method	$Se_{90}Sb_8Ag_2$	$Se_{90}Sb_6Ag_4$	$Se_{90}Sb_2Ag_8$
Augis Bennett's Method	1.35	1.16	0.66
Matusita and Sakka's method	1.38	1.19	0.71
Kissinger's Method	1.35	1.16	0.66

Table (10) Activation energy of crystallization E_{c2}(eV) in various glassy alloys of $Se_{90}Sb_{10-x}Ag_x$

Non-isothermal Method	$Se_{90}Sb_8Ag_2$	$Se_{90}Sb_6Ag_4$	$Se_{90}Sb_2Ag_8$
Augis Bennett's Method	1.80	1.71	-
Matusita and Sakka's method	1.85	1.70	-
Kissinger's Method	1.80	1.71	-

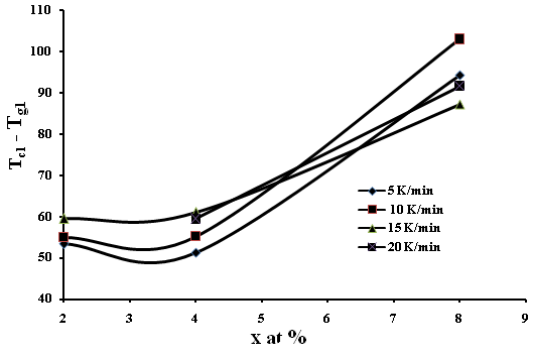

Fig. (11) T_{c1}–T_{g1} vs. atomic percentage of Ag in glassy $Se_{90}Sb_{10-x}Ag_x$

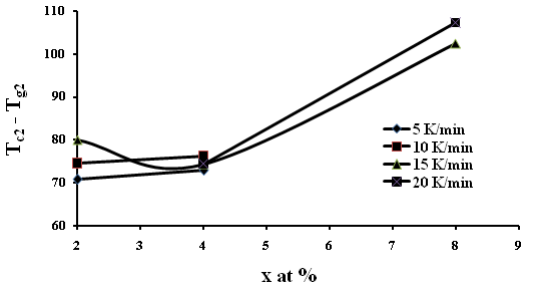

Fig. (12) T_{c2}–T_{g2} vs. atomic percentage of Ag in glassy $Se_{90}Sb_{10-x}Ag_x$

3.4 Activation Energy of Crystallization Kinetics

The activation energy of crystallization of each alloy has been calculated by three different methods Kissinger's method, Matusita-Sakka & Augis and Bennett used in the literature. According to Kissinger [35], peak temperature of crystallization T_c in terms of the heating rate β, can be expressed as:

$$Ln\left(\frac{\beta}{T_c^2}\right) = -\frac{E_c}{RT_c} + Constant \qquad (4)$$

This equation is used to calculate the activation energy of crystallization by plotting ln β/T_c^2 vs. $10^3/T_c$ curves (Figs. 13-17). Values calculated are given in Tables (9) and (10).

For the evaluation of E_c, Matusita and Sakka [36, 37] derived the following relation using the classical JMA theory:

$$Ln\beta = -\frac{E_c}{RT_c} + Constant \qquad (5)$$

This equation is used to calculate the activation energy of crystallization by plotting ln β vs. $10^3/T_c$ curve (Figs. 13-17). Values calculated are given in Tables (9) and (10).

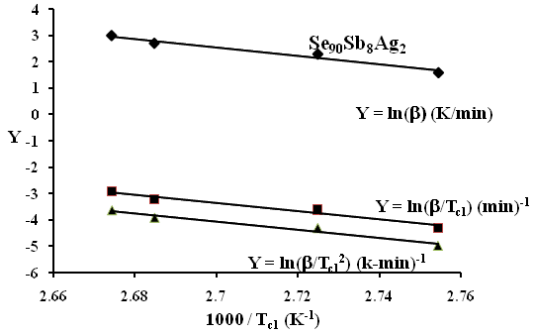

Fig. (13) Plots of ln (β/T_{c1}^2), ln (β/T_{c1}), ln (β) against $10^3/T_{c1}$ for $Se_{90}Sb_8Ag_2$

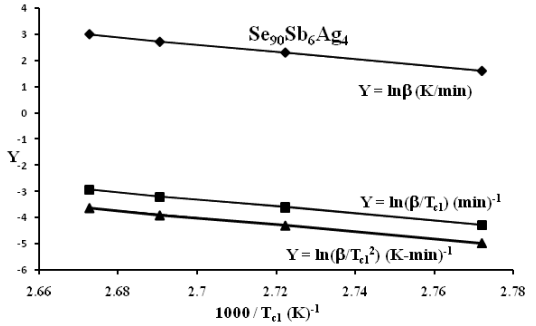

Fig. (14) Plots of ln (β/T_{c1}^2), ln (β/T_{c1}), ln (β) against $10^3/T_{c1}$ for $Se_{90}Sb_6Ag_4$

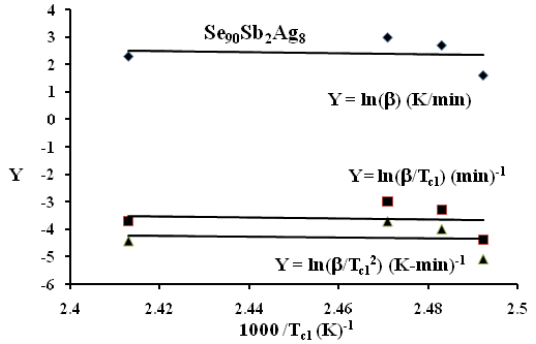

Fig. (15) Plots of ln (β/T_{c1}^2), ln (β/T_{c1}), ln (β) against $10^3/T_{c1}$ for $Se_{90}Sb_2Ag_8$

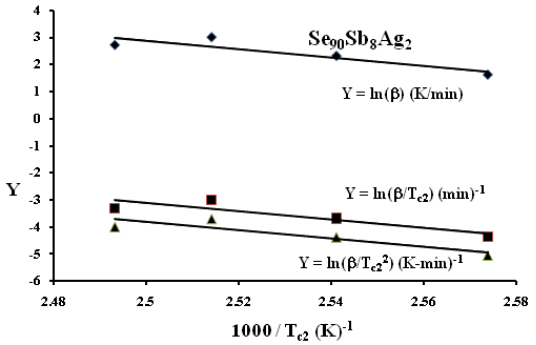

Fig. (16) Plots of ln (β/T_{c2}^2), ln (β/T_{c2}), ln (β) against $10^3/T_{c2}$ for $Se_{90}Sb_8Ag_2$

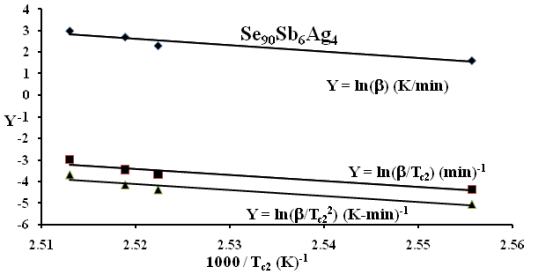

Fig. (17) Plots of ln (β/T_{c2}^2), ln (β/T_{c2}), ln (β) against $10^3/T_{c2}$ for $Se_{90}Sb_6Ag_4$

The activation energy of crystallization E_c can also be determined by an approximation method developed by Augis and Bennett [38]. The relation used by them is of the form:

$$Ln\left(\frac{\beta}{T_c}\right) = -\frac{E_c}{RT_c} + LnK_0 \qquad (6)$$

The activation energy of crystallization has been evaluated by this equation using the plots of ln β/T_c against $10^3/T_c$, as shown in Figs. (13-17). Values calculated are given in Tables (9) and (10).

Comparison of the E_c values, obtained from the three methods, shows that the values are in good agreement with each other. This means that one can use any of the three methods to obtain the activation energy of crystallization. The average value of E_{c1} and E_{c2} for each alloy has been given in the Tables (11) and (12). Figure (18) shows variation of E_{c1} with concentration of Ag.

Table (11) Average value of the activation energy of crystallization E_{c1}(eV) for various glassy alloys of $Se_{90}Sb_{10-x}Ag_x$

$Se_{90}Sb_8Ag_2$	1.36
$Se_{90}Sb_6Ag_4$	1.17
$Se_{90}Sb_2Ag_8$	0.68

Table (12) Average value of the activation energy of crystallization E_{c2} (eV) for various glassy alloys of $Se_{90}Sb_{10-x}Ag_x$

$Se_{90}Sb_8Ag_2$	1.82
$Se_{90}Sb_6Ag_4$	1.71
$Se_{90}Sb_2Ag_8$	-

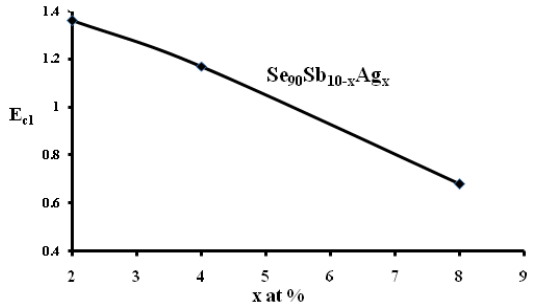

Fig. (18) E_{c1} vs. atomic percentage of Ag in glassy $Se_{90}Sb_{10-x}Ag_x$

4. Conclusion

DSC measurements have been performed for glassy alloys of $Se_{90}Sb_{10-x}Ag_x$. DSC scans of these alloys show double peaks at glass transition region as well as in crystallization region. Activation energy of glass transition E_g has been calculated by Moynihan's relation and Kissinger's relation. There is a good agreement between two values obtained from both the methods. Value of E_g is found to be decreased with increase in concentration of Ag.

The values of (T_c-T_g) is highest for the sample with 8 at % of Ag, Hence, one can conclude that the activation energy of glass transition process is related to thermal stability and GFT. Other workers have also found that the stable glass requires less activation energy for glass transition process [2, 36].

Activation energy of crystallization (E_c) has been calculated using three different methods. It has been found that E_c values obtained using the three different methods, i.e., Kissinger's method, Augis and Bennett's approximation method and Matusita and Sakka's method are in good agreement with each other. Thus one can use any of the three methods to calculate activation energy of crystallization. The activation energy of crystallization is found to decrease with increasing concentration of Ag.

References

[1] Moharram, A. H., Abu El-Oyoun, M., *J. Phys. D: Appl. Phys*., Vol.33, (2000) pp.700.
[2] Moharram, A. H., Rasheedy, M. S., *Phys. Stat. Sol. A*, Vol.169,(1998) pp.33.
[3] Qun Gao, Yi, Wang, W., *J. Non-Cryst. Solids*, Vol. 81, (1986) pp.129.
[4] Ligero, R. A., Vazquez, J., Villares, P., Jimenez-Garay, R., *Thermochim. Acta*, Vol.162, (1990) pp.427.
[5] Abdel-Rahim, M. A., *Physica B*, Vol.239, (1997) pp.238.
[6] Rysava, N., Spasov, T., Tichy, L., *J. Thermal Anal*., Vol. 32, (1987) pp.1015.
[7] Giridhar, A., Mahadevan, S., *J. Non-Cryst. Solids*, Vol.51, (1982) pp.305.
[8] Afify, N., *J. Non-Cryst. Solids*, Vol.128, (1991) pp.279.

[9] Strink, M. J., Zahara, A. M., *Thermochim. Acta*, Vol.298, (1997) pp.179.
[10] Chang, Y.Y., Chou, L.H., *Jpn. J. Appl. Phys. Part 2*, Vol.39 (4A), (2000) pp.294–296.
[11] Zhou, G.F., *Mater. Sci. Eng. A* , Vol.304–A306, (2001) pp.73.
[12] Chou, L.H., Chang, Y.Y., Chai, Y.C., Wang, S.Y., *J. Appl. Phys. Part 1*, Vol.40 (8), (2001) pp. 4924–4925.
[13] Li, J., Hou, L., Raun, H., Xie, Q., Gan, F., *Proc. SPIE Int. Soc. Opt. Eng*., Vol. 4085, (2001) pp. 125.
[14] Wagner, T., Frumar, M., Kasap, S.O., Vlcek, Mir., Vlcek, Mil., *J. Optoelectron. Adv. Mater*., Vol.3 (2), (2001) pp. 227.
[15] Gutwirth, J., Wagner, T., Kohoutek, T., Vlcek, Mir., Schroeter, S., Kovanda, V., Vlcek, Mil., Frumar, M., *J. Optoelectron. Adv. Mater*., Vol. 5 (5), (2003) pp.1139.
[16] Tanaka, K., *J. Non-Cryst. Solids*, Vol.164–166, (1993) pp.1179.
[17] Wagner, T., Jilkova, R., Frumar, M., Vicek, M., *Int. J. Electron*., Vol.77, (1994) pp.185.
[18] Tanaka, K., Itoh, M., Yoshida, N., Ohto, M., *J. Appl. Phys*., Vol.78, (1995) pp. 3895.
[19] Kawaguchi, T., Maruno, S., Elliott, S.R., J. Appl. Phys., Vol.79, (1996) pp.9096.
[20] Ohto, M., *Phys. Status Solidi A*, Vol.159, (1997) pp.461.
[21] Wagner, T., Frumar, M., Suskova, V., *J. Non-Cryst. Solids*, Vol.128, (1991) pp.197.
[22] Frumar, M., Polak, Z., Cernosek, Z., Frumarova, B., Wagner, T., *Chem. Paper*, Vol.57, (1997) pp. 310.
[23] Wagner, T., J. Optoelectron. Adv. Mater., Vol.4 (3), (2002) pp.717.
[24] Ramesh, K., Asokan, S., Sangunni, K.S., Gopal, E.S.R., *J. Phys. Chem. Solids*, Vol. 61, (2000) pp. 95.
[25] Frumar, M., Cernosek, Z., Jedelsky, J., Frumarova, B., wagner, T., *J. Optoelectron. Adv. Mater*., Vol.3 (2), (2001) pp.177.
[26] Tanaka, K., *J. Non-Cryst. Solids*, Vol.164–166, (1993) pp.1179.
[27] Wagner, T., Jilkova, R., Frumar, M., Vicek, M., *Int. J. Electron*., Vol.77, (1994) pp.185.
[28] Tanaka, K., Itoh, M., Yoshida, N., Ohto, M., *J. Appl. Phys*., Vol.78, (1995) pp. 3895.
[29] Kasap, S. O. and Juhaz, C., *J. Mater. Sci.*, Vol.24, (1986) pp.1329.
[30] Larmagnac , J. P., Grenet, J. and Michon, P., *J. Non-Cryst. Solids*, Vol.45, (1981) pp.157.
[31] Moynihan, C. T., Easteal, A. J., Wilder, J. and Tucker, J., *J. Phys. Chem.*, Vol.78, (1974) pp.267.
[32] Colemenero, J., Barandiaran, J. M., *J. Non-Cryst. Solids*, Vol. 30, (1978) pp.263.
[33] Kasap, S. O., Yannacopoulos, S., *Phys. Chem. Glasses*, Vol.31, (1990) pp. 71.
[34] Mehta, N., Tiwari, R.S., Kumar, A., *Mater. Res. Bull*., Vol.41, (2006) pp.1664.
[35] Kissinger, H. E., *Anal. Chem.*, Vol.29, (1997) pp.1702.
[36] Matusita, K., Sakka, S., *Phys. Chem. Glasses* , Vol.20, (1979) pp.81.
[37] Matusita, K., Sakka, S., *Bull Inst. Chem. Res. Kyoto Univ.*, Vol.59, (1981) pp.159.
[38] Augis, J.A., Bennett, J.E., *J. Them. Anal.*, Vol.13, (1978) pp.283.

